Cellular Physiology and Biochemistry

Cell Physiol Biochem 2018;49:706-716
DOI: 10.1159/000493036
Published online: 30 August, 2018
Accepted: 21 August, 2018

Original Paper

Effects of the Calcium-Activated Chloride Channel Inhibitors T16Ainh-A01 and CaCCinh-A01 on Cardiac Fibroblast Function

Xiang-qin Tian[a,b] Ke-tao Ma[a] Xian-wei Wang[b] Yang Wang[a] Zhi-kun Guo[b] Jun-qiang Si[a]

[a]Department of Physiology, Medical College of Shihezi University, Shihezi, [b]Henan Key Laboratory of Medical Tissue Regeneration, Xinxiang Medical University, Xinxiang, China

Key Words
Anoctamin-1 • Calcium-activated chloride channels • Cardiac fibroblasts • Cardiac fibrosis

Abstract
Background/Aims: Calcium-activated chloride channels (CaCCs) regulate numerous physiological processes including cell proliferation, migration, and extracellular matrix secretion. T16Ainh-A01 and CaCCinh-A01 are selective inhibitors of CaCCs. But it is unknown whether these two compounds have functional effects on cardiac fibroblasts (CFs). ***Methods:*** Primary CFs were obtained by enzymatic dissociation of cardiomyocytes from neonatal rat hearts. Intracellular Ca^{2+} ($[Ca^{2+}]_i$) and Cl^- ($[Cl^-]_i$) were measured using the fluorescent calcium indicators (Fluo-4 AM) and N-(ethoxycarbonylmethyl)-6-methoxyquinolinium bromide respectively. The expression of anoctamin-1 (ANO1) and α-smooth muscle actin (α-SMA) was detected by quantitative RT-PCR, immunofluorescence, and western blotting. A hydroxyproline assay was used to examine collagen secretion. Cell proliferation, cell cycle distribution, and cell migration were assessed by Cell Counting Kit-8, flow cytometry, and Transwell assays, respectively. ***Results:*** ANO1 was preferentially expressed on the nuclear membrane and partially within intracellular compartments around the nucleus. T16Ainh-A01 and CaCCinh-A01 displayed different inhibitory effects on $[Cl^-]_i$ in CFs. T16Ainh-A01 considerably decreased $[Cl^-]_i$ in the nucleus, whereas CaCCinh-A01 reduced $[Cl^-]_i$ in intracellular compartments around the nucleus, and both inhibitors exhibited a minimal effect on $[Ca^{2+}]_i$ in CFs. ANO1 and α-SMA expression levels were significantly repressed by CaCCinh-A01. T16Ainh-A01 showed a marked inhibitory effect on the mRNA levels of ANO1 and α-SMA, but had a negligible effect on ANO1 at the protein level. T16Ainh-A01 and CaCCinh-A01 led to the significant repression of cell proliferation, cell migration, and collagen secretion in CFs. ***Conclusion:*** Our findings

Dr. Jun-qiang Si
and Dr. Zhi-kun Guo

Department of Physiology, Medical College of Shihezi University
106 North St, Shihezi 832002 (China)
E-Mail sijunqiang11@hotmail.com; gzk@xxmu.edu.cn

indicate that T16Ainh-A01 and CaCCinh-A01 have the potential to inhibit the proliferation and collagen secretion of CFs and may serve as novel anti-fibrotic therapeutic drugs in the future.

Introduction

Cardiac fibroblasts (CFs) are located in interstitial and perivascular matrices and are essential for homeostasis [1, 2]. CFs are not only involved in extracellular matrix protein production, tissue repair, scar formation, inflammatory response, vasculogenesis, and tumorigenesis, but also have a role in myocardial remodeling, hypertensive heart disease, and heart failure [3, 4]. CFs actively participate in the regulation of cardiac physiological and pathological processes and thus represent pertinent targets for pharmacological approaches for cardiac diseases, which may point to novel therapeutic strategies [5].

Ion channels participate in diverse types of physiological activity integral to excitability, contraction, cell cycle, salt and water balance, and metastatic cascades, which play significant roles in the maintenance of tissue homeostasis during cell proliferation, differentiation, and apoptosis [6]. Normal cardiac electrophysiology relies on the dynamic and orchestrated operation of membrane ion channels and intracellular ion regulatory machineries [7]. The fibroblast properties of migration, secretion, and proliferation can be regulated by the activation of ion channels [5]. Meanwhile, chloride channels play essential roles in a variety of physiological functions including epithelial secretion, smooth muscle contraction, and sensory transduction [8]. Increasing evidence indicates that calcium-activated chloride channels (CaCCs) may participate in CF function [9-11] and be potential drug targets for the treatment of cardiovascular diseases [12].

Anoctamin-1 (ANO1; also known as TMEM16A, DOG1, ORAOV2, and TAOS2) is an eight-transmembrane domain protein functioning as a CaCC in the plasma membrane [13-15]. T16Ainh-A01 and CaCCinh-A01 are inhibitors of CaCCs that exhibit differences in their specific suppression of distinct cells. These compounds display poor selectivity for ANO1 and inhibition of CaCCs in vascular tissue in the concentration range that inhibits isolated conductance [16]. CaCCinh-A01 can inhibit ANO1-dependent chloride conductance and decrease the proliferation of ANO1-dependent cancer cell lines (Te11 and FaDu cells) by degrading ANO1 protein, whereas T16Ainh-A01 has no effect on ANO1 protein, although it exhibits anti-proliferative effects on cell lines (human airway and intestinal cells) with extremely low ANO1 expression levels [17, 18]. Furthermore, CaCCinh-A01 reduces cell viability, whereas T16Ainh-A01 has a minimal effect on the viability of colon cancer cells [19]. The inhibitory effects of T16Ainh-A01 and CaCCinh-A01 on CaCCs might be mediated by either the same or distinct signaling pathways in a cell type-specific manner. However, it is unclear whether both compounds influence the function of CFs. The aim of this study was to ascertain the effects of T16Ainh-A01 and CaCCinh-A01 on ANO1 expression, distribution of Ca^{2+} and Cl^-, cell proliferation, cell migration, and collagen secretion in CFs.

Materials and Methods

Animals

Neonatal Sprague–Dawley rats (male, 1–2 days old) were obtained from the Center of Experimental Animals of Xinxiang Medical University. Animal treatment was performed according to the guidelines of the Ministry of Science and Technology of the People's Republic of China ([2006]398) and approved by the Xinxiang Medical University Animal Care Committee (No. 030032).

Drugs and reagents

T16Ainh-A01(2-[(5-ethuy1-1,6-dihydro-4-methy1-6-oxo-2-pyrimidiny1)thio]-N-[4-4(4-methoxypheny1)-2-thiazoyoly1]acetamide) and CaCCinh-A01 (6-(1, 1-dimethylethy1)-2-[(2-furanylcarbonyl)amino]-4, 5,6, 7-tetrahydrobenzo [b]thiophene-3-carboxylic acid) were purchased from

Sigma-Aldrich (St. Louis, MO, USA). Stock solutions of the above reagents (20 mM) were prepared using dimethyl sulfoxide (DMSO) as a solvent, and stored at -20°C until use. All work solutions were prepared freshly from stock solutions before each experiment and not exposed to light. CFs were treated with 10 μM T16Ainh-A01, 30 μM CaCCinh-A01, and matching volumes of DMSO (0.1% v/v).

CF isolation and culture

Primary CFs were obtained from the left ventricles of neonatal Sprague–Dawley rats by enzymatic dissociation and selective plating methods as described previously [20, 21]. In brief, neonatal rats were euthanized by CO_2 asphyxiation. Their hearts were excised under sterile conditions and cut into approximately 1-mm^3 pieces. The tissues were rinsed in Hanks' balanced salt solution prior to digestion with 0.1% (w/v) collagenase type II (Sigma-Aldrich) in Hanks' balanced salt solution without Ca^{2+} and Mg^{2+} for 20 min and then 0.125% (*w/v*) trypsin (Sigma-Aldrich) for 10 min at 37 °C in a shaking bath. After the addition of Dulbecco's modified Eagle's medium (DMEM: ThermoFisher Scientific, Shanghai, China), the samples were filtered with a 70-μm metal mesh filter and centrifuged for 10 min at 1000 × *g*. The filtered particles were resuspended in DMEM supplemented with 10% (v/v) fetal bovine serum (Thermo Fisher Scientific) and 1% penicillin/streptomycin (Solarbio, Beijing, China). Finally, the CFs were separated from myocytes and other cells by selective plating (adherence after 45 min in culture). The identity and purity of CFs were assessed by characteristic morphology and immunofluorescence staining for vimentin. CFs from the third passage were used in the subsequent experiments.

Measurements of intracellular Ca^{2+} and Cl^-

The effects of T16Ainh-A01 and CaCCinh-A01 on intracellular Ca^{2+} ($[Ca^{2+}]_i$) were monitored by imaging Fluo-4 AM fluorescence according to the manufacturer's instructions. Briefly, Fluo-4 AM was solubilized in anhydrous DMSO and then diluted with HEPES-buffered saline (HBS). CFs with 60% confluence were washed 3 times with HBS and incubated with 10 μM T16Ainh-A01, 30 μM CaCCinh-A01, or 0.1% DMSO for 48 h. Following washing 3 times with HBS, the cells were incubated with Fluo-4 AM (2.5 μM, pH 7.4) for 45 min at 37°C and washed 3 times with HBS. De-esterification of Fluo-4 AM was extended for an additional 20 min. The excitation and emission wavelengths of Fluo-4 AM were 488 and 520 nm, respectively. Background fluorescence measured prior to loading was subtracted from the measured emissions. Images were recorded with a laser scanning confocal microscope (LSM 510; Zeiss, Oberkochen, Germany).

The effects of T16Ainh-A01 and CaCCinh-A01 on intracellular Cl^- ($[Cl^-]_i$) were measured with the chloride probe N-(ethoxycarbonylmethyl)-6-methoxyquinolinium bromide (MQAE; Beyotime, Shanghai, China) as per the manufacturer's instructions. In brief, CFs at 60% confluence were washed 3 times with Krebs-HEPES buffer and incubated with 10 μM T16Ainh-A01, 30 μM CaCCinh-A01, or 0.1% DMSO for 48h. Then, cells were incubated with 10 mM MQAE for 1h at 37°C in HEPES buffer before they were transferred to a perfusion chamber. The excitation and emission wavelengths of Fluo-4 AM were 355 and 460 nm, respectively. Images were recorded with a laser scanning confocal microscope (LSM 510; Zeiss).

RNA extraction and quantitative real-time RT-PCR (qRT-PCR)

Primary CFs were isolated as described above, and approximately 1.0 × 10^6 cells were collected with a cell sorter. Total RNA was extracted from CFs with the TRIzol reagent (ThermoFisher Scientific, Shanghai, China) and quantified by assessing their optical densities at 260 and 280 nm using a NanoDrop ND-100 (LabTech, Beijing, China). Reverse transcription was performed according to the manufacturer's protocol (Thermo Fisher Scientific, Shanghai, China). In brief, 1 μL total RNA (1-2 μg) was added to reaction mixture containing 5×reaction buffer, 10 mM dNTP mix, 1 μL oligo$(dT)_{18}$ primer, 20 U RNase inhibitor, and 200 U M-MuLV reverse transcriptase to a final volume of 20 μL cDNA was synthesized at 42°C for 1h. Remaining enzymes were heat-inactivated at 70°C for 5 min.

qRT-PCR was carried out with SYBR Premix Ex Taq™ II SYBR Premix Ex (TAKARA Bio, Inc., Dalian, China). All reactions during the process were amplified in triplicate on a LightCycler® System (Roche, Switzerland) in a total volume of 10 μL containing 5 μL of SYBR green master mix, 0.8 μL of primer, 1 μL diluted cDNA, and 3.2 μL H_2O. The samples were pre-incubated at 95°C for 10min, followed by 45 cycles of 95°C for 15s, 61°C for 15s, and 72°C for 30s. The ratio between the amount of target genes and endogenous standard (GAPDH) was calculated for each sample, and analyses were performed in triplicate, yielding transcriptional quantification of gene products relative to GAPDH.

The primers for the target genes were designed with Oligo 6.0 software (Molecular Biology Insights, Inc., Cascade, CO, USA), and synthesis was performed by Sangon Biotech Co., Ltd. (Shanghai, China). Primer sequences and expected amplicon sizes of the target genes are provided in Table 1.

Table 1. Oligonucleotide primers for qRT-PCR in this study. GAPDH, glyceraldehyde-3-phosphate dehydrogenase

Primer	Gene Accession No.	Oligonucleotide Sequences (5′-3′)	Amplicon Size (bp)
ANO1F	NM_001107564	ATTTCACCAATCTTGTCTCCATCA	424
ANO1R		TGATAACTCCAAGAACGATTGCA	
collagen IF	NM_053304.1	TGGCCCCATTGGTAACGTTG	130
collagen IR		TCCAGCATTTCCAGAGGGACC	
collagen IIIF	NM_032085.1	GAGCGGAGAATACTGGGTTGA	289
collagen IIIR		TGTAATGTTCTGGGAGGCCC	
α-SMAF	NM_031004.2	CATCACCAACTGGGACGACA	96
α-SMAR		TCCGTTAGCAAGGTCGGATG	
GAPDHF	NM_017008.4	ACACCCACTCCTCCACCTTT	166
GAPDHR		TTACTCCTTGGAGGCCATGT	

Protein extraction and western blot analysis

Different groups of CFs were harvested into a lysis buffer (20 mM Tris-base, 137 mM NaCl, 10% glycerol, 1% Triton X-100, 2 mM EDTA, and 1 μL/mL protease inhibitor). The lysates were centrifuged at 4 °C and 13000 × *g* for 30 min. The supernatant was collected, and protein concentrations were measured with a bicinchoninic acid protein assay kit (Beyotime). The proteins were separated by 8% sodium dodecyl sulfate–polyacrylamide gel electrophoresis and transferred to a nitrocellulose membrane. After blocking in tris-buffered saline (TBS) containing 5% non-fat milk, the membranes was incubated with appropriate primary antibodies consisting of rabbit polyclonal anti-ANO1 (1:1; Abcam; Cambridge, UK) or mouse monoclonal anti-α-smooth muscle actin (α-SMA; Sigma-Aldrich) overnight at 4 °C. After incubation, the membrane was rinsed 3 times with TBS Tween 20 (TBST; 150 mM NaCl, 20 mM Tris-base, and 0.05% Tween 20) for 10 min, and incubated with secondary antibodies at room temperature for 1–2 h. The membrane was washed twice with TBST for 10 min per wash and once with TBS for 10 min. Protein bands were visualized on an ECL system (Amersham Biosciences, Piscataway, NJ, USA) and the results were analyzed with Image-Pro Plus 6.0 software.

Immunofluorescence staining

CFs were placed in 24-well plates at a density of 2.0 × 10^5 cells/mL and 500 μL/well. The cells were fixed with 10% formalin for 20 min when they reached 80% confluence. After washing 3 times with phosphate-buffered saline (PBS), The cells were permeabilized in 0.1% Triton X-100 for 20 min and blocked with 5% bovine serum albumin in TBS for 1 h. The cells were incubated with appropriate primary antibodies at 4 °C overnight, and then with appropriate second antibodies (FITC-conjugated affiniPure goat anti-mouse lgG [H+L], 1:500; Cy™ 3-conjugated affiniPure goat anti-rabbit lgG [H+L], 1:500; Jackson ImmunoResearch Laboratories, Inc., West Grove, PA, USA) for 2 h at room temperature. The nuclei were stained with 4′,6-diamidino-2-phenylindole (Sigma-Aldrich) for 10 min. Protein localization in the cells was observed and captured with a laser scanning confocal microscope (LSM 510; Zeiss).

Measurement of collagen secretion in rat CFs by hydroxyproline assay

The effects of the inhibitors on collagen secretion by CFs were assessed by using a hydroxyproline assay kit (Jiancheng Bioengineering Institute, Nanjing, China) according to the manufacturer's instructions. Collagen content in the culture medium was calculated based on the absorbance, which was normalized using a blank control. Average hydroxyproline content was normalized by OD value representing cell number.

Cell cycle analysis

Cell cycle distribution was detected with a propidium iodide cell cycle kit (MultiSciences Biotech, Hangzhou, China) according to the manufacturer's instructions. Briefly, the cells were detached using 0.125% (w/v) trypsin, collected by centrifugation for 10 min at 1000 × g, washed with cold PBS, and fixed overnight in 70% ice-cold ethanol. The fixed cells were washed twice with PBS and treated with 10 μg/mL RNase I for 30 min at 37 °C before staining with 50 μg/mL propidium iodide. The stained cells were analyzed by flow cytometry (Becton Dickinson, Franklin Lakes, NJ, USA).

Cell proliferation assay

The cells were seeded in 96-well plates at a density of 1.0×10^5 cells/well in 100 µL culture medium and maintained in a CO_2 incubator at 37 °C for 24 h. Cell proliferation was measured with a Cell Counting Kit-8 (CCK-8; Beyotime). Briefly, 10 µL of the CCK-8 solution was added to each well of the plate, and cells were incubated for 2 h at 37 °C. Absorbance was measured at 450 nm with a microplate reader (Thermo Fisher Scientific). In this experiment, cell viability was determined at 48 h after treatment with 10 µM T16Ainh-A01, 30 µM CaCCinh-A01, or 0.1% DMSO (control).

Cell migration assay

Transwell inserts with 8.0-µm pore size (Corning, Inc., Corning, NY, USA) were used to assess CF migration. Prior to seeding into the upper compartments of the inserts (2.0×10^5 cells/well), CFs were pre-starved in serum-free medium for 24 h. The cells were cultured in the upper compartments for 24 h, the non-invasive cells were removed from the upper surface of each insert, and the migrated cells were fixed with methanol, stained with 1% crystal violet, and counted using a light microscope in 5 random visual fields at a magnification of 100×.

Statistical analysis

All data are expressed as the mean ± standard error of the mean. Statistical analyses were performed using GraphPad Prism software (GraphPad Software, Inc., San Diego, CA, USA). An unpaired Student's *t*-test or one-way analysis of variance followed by Bonferroni's multiple comparisons *post hoc* test was used for statistical comparisons. Differences were considered statistically significant at $p < 0.05$.

Results

Identification of CFs and expression of ANO1 in CFs

CFs stained positive for vimentin and were typically spindle or triangle shaped under a light microscope (Fig. 1A). Next, we investigated the distribution of ANO1 protein in CFs by immunostaining. As shown in Fig. 1B, ANO1 expression was predominantly located on the nuclear membrane and partially around the nucleus, especially in CFs in the mitotic phase. To our knowledge, this is the first report on the cellular localization of ANO1 protein in CFs.

T16Ainh-A01 and CaCCinh-A01 reduce $[Cl^-]_i$ in CFs but do not affect $[Ca^{2+}]_i$

As shown in Fig. 2A (upper) and Fig. 2B, there was no significant difference of $[Ca^{2+}]_i$ among the cells treated with 10 µM T16Ainh-A01, 30 µM CaCCinh-A01 and 0.1% DMSO, respectively ($p > 0.05$). This indicates that neither compounds had an effect on $[Ca^{2+}]_i$. The novel fluorescent indicator MQAE was used to measure $[Cl^-]_i$ in CFs. High fluorescence intensity of MQAE reflects low $[Cl^-]_i$, while low fluorescence intensity reflects high $[Cl^-]_i$. As shown in Fig. 2A (lower panel), T16Ainh-A01 inhibited Cl^- influx into the nucleus, while CaCCinh-A01 led to a decrease of Cl^- content in intracellular compartments around the nucleus $[Cl^-]_i$ was significantly decreased in CFs treated with both T16Ainh-A01 and CaCCinh-A01 (both $p < 0.01$, $n = 5$, Fig. 2C).

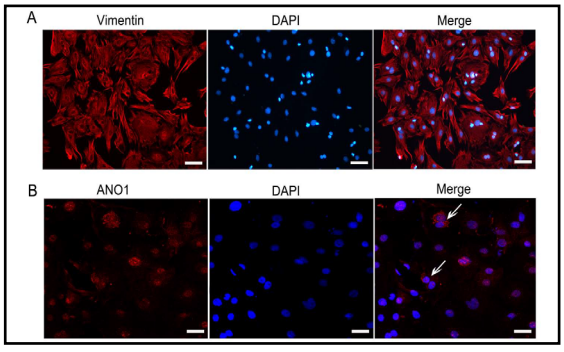

Fig. 1. Identification of the phenotype of rat cardiac fibroblasts (CFs) and the expression of ANO1. (A) vimentin immunostaining (red). Scale bar = 50 µm. (B) ANO1 immunostaining (red). ANO1 localized predominantly at the nuclear membrane and partially within intracellular compartments around nucleus in CF, especially at mitotic phase (indicated by white arrows). Scale bar = 25 µm.

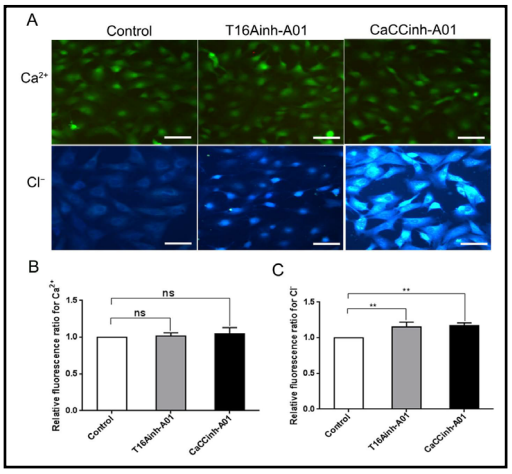

Fig. 2. The effects of T16Ainh-A01 and CaCCinh-A01 on intracellular Ca^{2+} and Cl^- concentrations in primary CFs. (A) intracellular Ca^{2+} and Cl^- were detected by Fluo 4-AM (upper) and MQAE probe staining (lower), respectively. (B-C) quantitative analysis of intracellular Ca^{2+} and Cl^- density. Data are expressed as mean ± SEM; n=5; ns, no significant difference, **P<0.01 represents statistical comparisons of inhibitors versus controls. Scale bar = 25 μm.

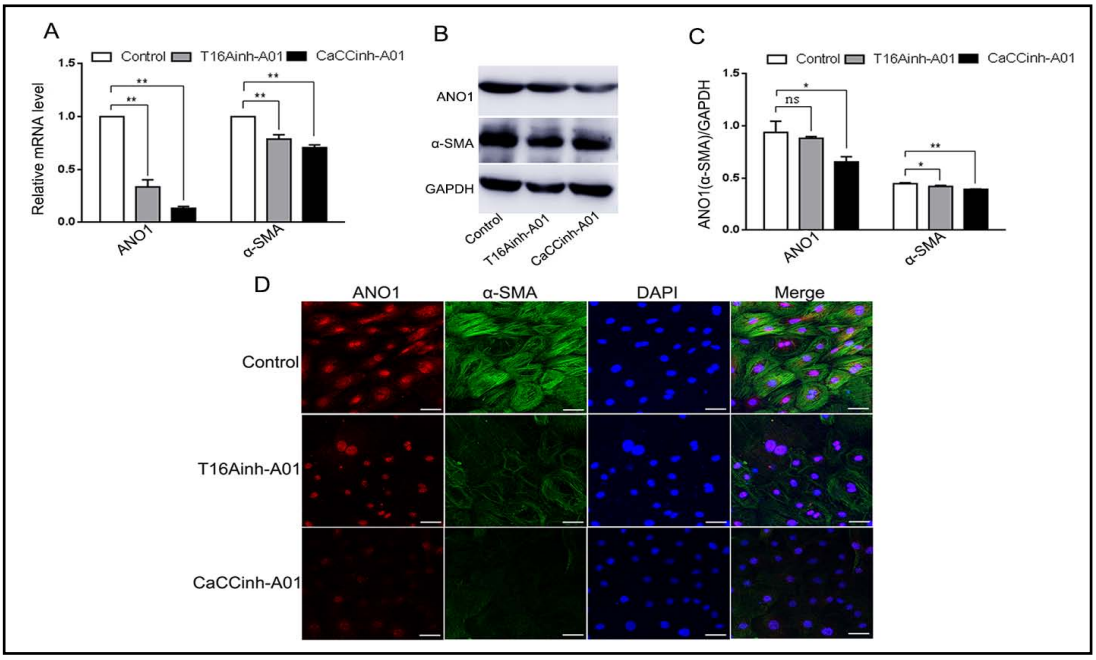

Fig. 3. The expression of ANO1 and α-SMA in rat CFs after treatment with T16Ainh-A01 and CaCCinh-A01 for 48 h. (A) qRT-PCR data show the mRNA expressions of ANO1 and α-SMA. (B-C) Western blot data show the protein expressions of ANO1 and α-SMA. (D) expression of ANO1 and α-SMA by immunoflurescence staining. ANO1 and α-SMA were red and green, respectively, and nuclei were identified by DAPI staining (blue). ns, no significant difference; *p<0.05, vs. control; **p<0.01, vs. control. Scale bar = 40 μm.

Effect of T16Ainh-A01 and CaCCinh-A01 on ANO1 and α-SMA expression in rat CFs

When the primary CFs were treated with 10 μM T16Ainh-A01, the expression of ANO1 and α-SMA mRNA was markedly decreased compared with control ($p < 0.01$ for both ANO1 and α-SMA, $n = 5$, Fig. 3A). The inhibitory effects of 30 μM CaCCinh-A01 on ANO1 and α-SMA mRNA expression were even greater ($p < 0.01$, $n = 5$, Fig. 3A). Western blot analysis showed that the protein expressions of ANO1 and α-SMA protein in CFs was markedly reduced in CFs after treatment with CaCCinh-A01 ($p < 0.05$ for ANO1, $p < 0.01$ for α-SMA, $n = 5$). T16Ainh-A01 also reduced the protein expression of α-SMA, but did not affect ANO1 protein expression ($p > 0.05$, $n = 5$, Fig. 3B and C). Consistent with the western blot data, immunofluorescence staining also showed that CaCCinh-A01 caused comparatively weaker fluorescent signals for ANO1 and α-SMA in CFs compared with T16Ainh-A01 (Fig. 3D).

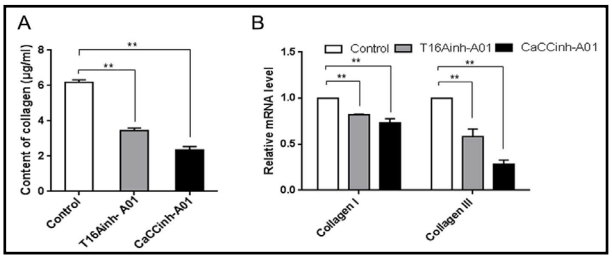

Fig. 4. Collagen secretion from CFs after treatment with T16Ainh-A01 and CaCCinh-A01 for 48 h. (A) collagen content (measured by hydroxyproline assay) in different groups. (B) relative mRNA expressions of collagen Ⅰ and collagen Ⅲ (measured by qRT-PCR) in different groups. Data are expressed as mean ± SEM, **p<0.01, vs. control.

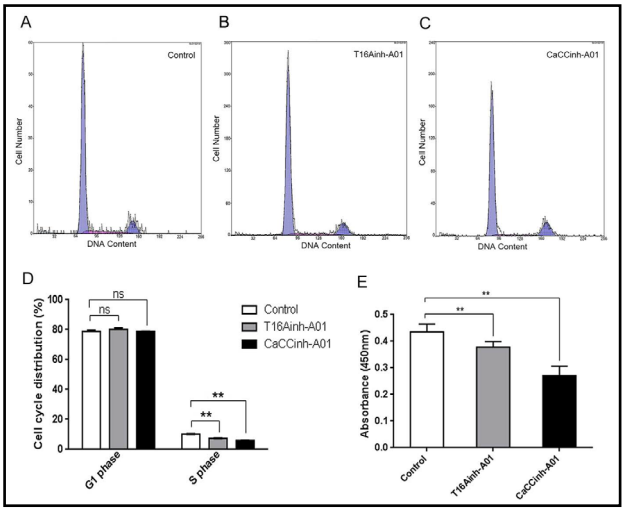

Fig. 5. The effects of T16Ainh-A01 and CaCCinh-A01 on proliferation and cell cycle of rat CFs. (A-D) flow cytometric data show cell cycle phases in different groups of CFs. (E) cell proliferation (measured by CCK-8 assay). CFs in T16Ainh-A01 and CaCCinh-A01 groups were treated with T16Ainh-A01 (10 μM) and CaCCinh-A01 (30 μM) for 48 h, respectively. Treatments with T16Ainh-A01 and CaCCinh-A01 markedly arrested the cells at G1 phase and caused the reduction of cells at S phase. Data are expressed as mean ± SEM; ns, no significant difference; **p<0.01, vs. control.

T16Ainh-A01 and CaCCinh-A01 reduced the secretion of collagen from CFs

The amounts of secreted collagen (μg/mL) secreted were significantly lower in the T16Ainh-A01 and CaCCinh-A01-treated groups compared with the control group (T16Ainh-A01 3.453 ± 0.137 vs. 6.180 ± 0.146 of control, $p < 0.01$, $n = 5$; CaCCinh-A01 2.355 ± 0.187 vs. 6.180 ± 0.146 of control, $p < 0.01$, $n = 5$, Fig. 4A). Both CaCCinh-A01 and T16Ainh-A01 displayed significant inhibitory effects on the mRNA expression of types I and type III collagen (both $p < 0.01$, $n = 5$, Fig. 4B).

T16Ainh-A01 and CaCCinh-A01 inhibited CF proliferation and cell cycle progression

Both compounds inhibited cell cycle progression at the G1 phase and there was a significant decrease in the number of cells at the S phase. The percentages of cells at the G1 phase were 80.18 ± 0.49% and 78.87 ± 0.07% (vs. 78.99 ± 0.31% in control, $n = 3$) in the T16Ainh-A01- and CaCCinh-A01-treated groups, respectively. The percentages of the cells at the S phase decreased significantly from 10.18 ± 0.06% in the control group to 7.41 ± 0.02% ($n = 3$) and 6.04% ± 0.04% ($n = 3$) in the T16Ainh-A01 and CaCCinh-A01-treated groups (both $p < 0.01$, $n = 3$, Fig. 5A-D), respectively. Both T16Ainh-A01 and CaCCinh-A01 exhibited significant inhibitory effects on CF proliferation (T16Ainh-A01 absorbance 0.378 ± 0.0097 vs. 0.435 ± 0.0133 of control, $p < 0.01$, $n = 3$; CaCCinh-A01 absorbance 0.271 ± 0.0155 vs. 0.435 ± 0.0133 of control, $n = 3$, Fig. 5E).

T16Ainh-A01 and CaCCinh-A01 inhibited CF migration

The migration of CFs was measured by a Transwell migration assay. As shown in Fig. 6A and B, both T16Ainh-A01 and CaCCinh-A01 significantly inhibited the migration of rat CFs (both $p < 0.01$, $n = 5$).

Discussion

We showed for the first time that ANO1 was mainly localized in the nuclear membrane of the rat CFs. T16Ainh-A01 inhibited Cl^- influx into the nucleus, and CaCCinh-A01 caused a global decrease of Cl^- content. Our findings demonstrated that both inhibitors suppressed CF proliferation by inducing cell cycle arrest at the G1 phase, and also inhibited cell migration and collagen secretion of CFs.

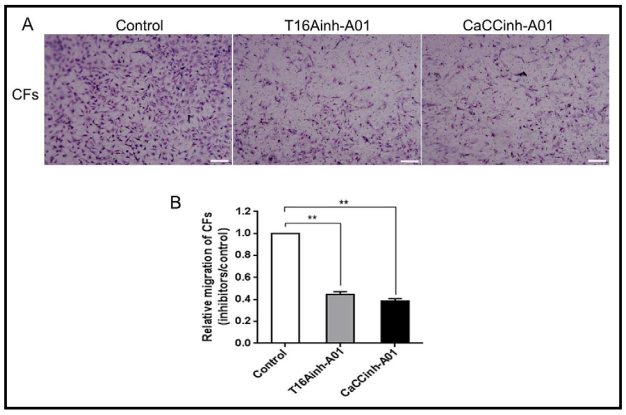

Fig. 6. The effects of T16Ainh-A01 and CaCCinh-A01 on cell migration of rat CFs. (A) representative staining images for transmigrated cells. The cells in T16Ainh-A01 and CaCCinh-A01 groups were treated with T16Ainh-A01 (10 μM) or CaCCinh-A01 (30 μM) for 24 h. (B) the calculated relative ratios of the transmigrated cells. Data are expressed as mean ± SEM, **p<0.01, vs. control. Scale bar = 100 μm.

ANO1 is a key factor for CaCC-mediated conductance [13-15]. ANO1 localization may vary in distinct cell types [22-24]. In dorsal root ganglion neurons. ANO1 is predominately located in the cell membrane [25]. A recent study on the expression, localization, and distribution of ANO1 in murine ventricular tissues and myocytes revealed that ANO1 was evenly distributed in the left ventricular epicardium and endocardium and localized abundantly to the plasma membrane of murine ventricular myocytes [24]. However, in cultured uterine smooth muscle cells, ANO1 was found to be expressed mainly in the cytoplasm adjacent to the nucleus [26]. In this study, we demonstrated for the first time that ANO1 was predominantly expressed on the nuclear membrane of CFs and partially within intracellular compartments around the nucleus. This result challenges a previous study demonstrating that ANO1 was highly expressed in the cytoplasmic membrane of rat CFs [11]. Notably, ANO1 expression was extremely low in freshly isolated CFs, but it was significantly enhanced at 48 h after CF attachment to the culture dish (data not shown). The expression pattern of ANO1 indicates that it not only plays an important role in the modulation of Cl^- flux through CaCCs but also has additional biological functions.

Several studies have confirmed that T16Ainh-A01 and CaCCinh-A01 exert their inhibitory effects in a dose-dependent manner [18, 19, 27, 28]. T16Ainh-A01 (10 μM) strongly inhibits TMEM16A-mediated iodide influx and completely blocks CaCC conductance in salivary gland cells. CaCCinh-A01, with fitted IC_{50} values of 2.1 μM, can block ANO1-encoded CaCC currents at a high concentration (30 μM) but has no effect on $[Ca^{2+}]_i$ in human intestinal epithelial cells [18, 29]. In the present study, we also found that T16Ainh-A01 and CaCCinh-A01 exerted their inhibitory effects in a dose-dependent manner. Exposure to 20 μM T16Ainh-A01 and 60 μM CaCCinh-A01 was cytotoxic, as manifested by cells death and morphology changes (data not shown), whereas 10 μM T16Ainh-A01 and 30 μM CaCCinh-A01 did not show obvious cytotoxicity and strongly inhibited $[Cl^-]_i$ and the proliferation of CFs.

It has been reported that T16Ainh-A01 can inhibit ANO1-dependent chloride conductance in cells but does not affect ANO1 expression in airway and intestinal epithelia [18], whereas CaCCinh-A01 inhibits ANO1-dependent cell proliferation by promoting the endoplasmic reticulum-associated proteasomal degradation of ANO1 in ANO1-dependent cell lines [17]. It has also been reported that ANO1 plays an important role in the modulation of cardiac fibrosis and is a potential therapeutic target for cardiac fibrosis of myocardial infarction [11]. However, little is known about the effects of T16Ainh-A01 and CaCCinh-A01 on ANO1 expression in CFs. In the present study, we found that CaCCinh-A01 significantly inhibited ANO1 expression, whereas T16Ainh-A01 did not have a significantly effect on the protein level of ANO1, although both inhibitors could suppress CF proliferation, migration,

and collagen secretion. We speculate that T16Ainh-A01 may affect CF functions by simply inhibiting CaCCs, whereas CaCCinh-A01 exerts its inhibitory effects on CFs by not only closing CaCCs but also by inactivating ANO1. The precise mechanisms responsible for the actions of these inhibitors require further investigation.

Further, we evaluated the effects of T16Ainh-A01 and CaCCinh-A01 on the expression of α-SMA, a typical marker of myofibroblasts, which are closely associated with cardiac fibrosis [30, 31], and demonstrated that both inhibitors reduced α-SMA expression at the mRNA and protein level. The synthesis and secretion of collagen are the main functions of CFs, which play a pivotal role in the myocardial repair process [32]. Our results showed that CaCCinh-A01 and T16Ainh-A01 could significantly inhibit the secretion of collagen from CFs. These findings indicate that both inhibitors may play roles in modulating the development of cardiac fibrosis.

Chloride channels provide the main electrical shunt for the acidification of most organelles of the secretory and endocytic pathways and play essential roles in a variety of physiological and pathophysiological processes in many diseases [33]. CaCCinh-A01 and T16Ainh-A01 are the most potent inhibitors of calcium-activated Cl^- conductance and are typically used to examine the contributions of CaCCs/ANO1 in physiological models, although their specificity remains uncertain [8, 16]. CaCCinh-A01 can completely block CaCC current in human bronchial and intestinal epithelial cells, whereas T16Ainh-A01 poorly inhibits total CaCC current, but blocks an initial agonist-stimulated transient chloride current [34]. CaCCs are activated by an increases in the level of intracellular free calcium, and Cl^- flux through CaCCs is generally thought to be driven by ANO1 or ANO2 [8]. An important finding of this study was that T16Ainh-A01 inhibited Cl^- influx into the nucleus, while CaCCinh-A01 reduced Cl^- level in intracellular compartments around the nucleus. These results extend our knowledge of the mechanisms of action of two new inhibitors and lay the foundation for the future development of anti-fibrotic drugs.

Conclusion

Overall, this study provides novel information about the effects of T16Ainh-A01 and CaCCinh-A01 on CFs. Both inhibitors can suppress cell proliferation, cell migration, and collagen secretion from CFs, suggesting that they have therapeutic potential for the treatment of cardiac fibrosis. However, their involvement and utility in heart disease remain unclear and require further study.

Acknowledgements

Authors would like to thank Dr Magomed Khaidakov from University of Arkansas for Medical Sciences, for revising the paper and advice in the work. The authors gratefully acknowledge funding support by the National Natural Science Foundation of China (Grant No. 81560081).

Disclosure Statement

The authors declare to have no conflict of interests.

References

1 Travers JG, Kamal FA, Robbins J, Yutzey KE, Blaxall BC: Cardiac fibrosis: the fibroblast awakens. Circ Res 2016;118:1021-1040.

2 Shi H, Zhang X, He Z, Wu Z, Rao L, Li Y: Metabolites of hypoxic cardiomyocytes induce the migration of cardiac fibroblasts. Cell Physiol Biochem 2017;41:413-421.
3 Chistiakov DA, Orekhov AN, Bobryshev YV: The role of cardiac fibroblasts in post-myocardial heart tissue repair. Exp Mol Pathol 2016;101:231-240.
4 Deng P, Chen L, Liu Z, Ye P, Wang S, Wu J, Yao Y, Sun Y, Huang X, Ren L, Zhang A, Wang K, Wu C, Yue Z, Xu X, Chen M: MicroRNA-150 inhibits the activation of cardiac fibroblasts by regulating c-Myb. Cell Physiol Biochem 2016;38:2103-2122.
5 Chacar S, Fares N, Bois P, Faivre JF: Basic signaling in cardiac fibroblasts. J Cell Physiol 2017;232:725-730.
6 Liu W, Lu M, Liu B, Huang Y, Wang K: Inhibition of Ca^{2+}-activated Cl^- channel ANO1/TMEM16A expression suppresses tumor growth and invasiveness in human prostate carcinoma. Cancer Lett 2012;326:41-51.
7 Nguyen MN, Kiriazis H, Gao XM, Du XJ: Cardiac fibrosis and arrhythmogenesis. Compr Physiol 2017;7:1009-1049.
8 Friard J, Tauc M, Cougnon M, Compan V, Duranton C, Rubera I: Comparative Effects of Chloride Channel Inhibitors on LRRC8/VRAC-Mediated Chloride Conductance. Front Pharmacol 2017;8:328.
9 El Chemaly A, Norez C, Magaud C, Bescond J, Chatelier A, Fares N, Findlay I, Jayle C, Becq F, Faivre JF, Bois P: ANO1 contributes to angiotensin-II-activated Ca^{2+}-dependent Cl^- current in human atrial fibroblasts. J Mol Cell Cardiol 2014;68:12-19.
10 He ML, Liu WJ, Sun HY, Wu W, Liu J, Tse HF, Lau CP, Li GR: Effects of ion channels on proliferation in cultured human cardiac fibroblasts. J Mol Cell Cardiol 2011;51:198-206.
11 Gao Y, Zhang YM, Qian LJ, Chu M, Hong J, Xu D: ANO1 inhibits cardiac fibrosis after myocardial infraction via TGF-beta/smad3 pathway. Sci Rep 2017;7:2355.
12 Gourdie RG, Dimmeler S, Kohl P: Novel therapeutic strategies targeting fibroblasts and fibrosis in heart disease. Nat Rev Drug Discov 2016;15:620-638.
13 Yang YD, Cho H, Koo JY, Tak MH, Cho Y, Shim WS, Park SP, Lee J, Lee B, Kim BM, Raouf R, Shin YK, Oh U: TMEM16A confers receptor-activated calcium-dependent chloride conductance. Nature 2008;455:1210-1215.
14 Schroeder BC, Cheng T, Jan YN, Jan LY: Expression cloning of TMEM16A as a calcium-activated chloride channel subunit. Cell 2008;134:1019-1029.
15 Caputo A, Caci E, Ferrera L, Pedemonte N, Barsanti C, Sondo E, Pfeffer U, Ravazzolo R, Zegarra-Moran O, Galietta LJ: TMEM16A, a membrane protein associated with calcium-dependent chloride channel activity. Science 2008;322:590–594.
16 Boedtkjer DM, Kim S, Jensen AB, Matchkov VM, Andersson KE: New selective inhibitors of calcium-activated chloride channels-T16A(inh)-A01, CaCC(inh)-A01 and MONNA-what do they inhibit? Br J Pharmacol 2015;172:4158-4172.
17 Bill A, Hall ML, Borawski J, Hodgson C, Jenkins J, Piechon P, Popa O, Rothwell C, Tranter P, Tria S, Wagner T, Whitehead L, Gaither LA: Small molecule-facilitated degradation of ANO1 protein: a new targeting approach for anticancer therapeutics. J Biol Chem 2014;289:11029-11041.
18 Namkung W, Phuan PW, Verkman AS: TMEM16A inhibitors reveal TMEM16A as a minor component of calcium-activated chloride channel conductance in airway and intestinal epithelial cells. J Biol Chem 2011;286:2365-2374.
19 Guan L, Song Y, Gao J, Gao J, Wang K: Inhibition of calcium-activated chloride channel ANO1 suppresses proliferation and induces apoptosis of epithelium originated cancer cells. Oncotarget 2016;7:78619-78630.
20 Rhaleb N, Peng H, Harding P, Tayeh M, LaPointe M, Carretero O: Effect of N-acetyl-seryl-aspartyl-lysyl-proline on DNA and collagen synthesis in rat cardiac fibroblasts. Hypertension 2001;37:827-832.
21 Chang Y, Guo K, Li Q, Li C, Guo Z, Li H: Multiple directional differentiation difference of neonatal rat fibroblasts from six organs. Cell Physiol Biochem 2016;39:157-171.
22 Tian Y, Schreiber R, Kunzelmann K: Anoctamins are a family of Ca^{2+}-activated Cl^- channels. J Cell Sci 2012;125:4991-4998.
23 Rock J, Futtner C, Harfe B: The transmembrane protein TMEM16A is required for normal development of the murine trachea. Dev Biol 2008;321:141–149.
24 Ye Z, Wu MM, Wang CY, Li YC, Yu CJ, Gong YF, Zhang J, Wang QS, Song BL, Yu K, Hartzell HC, Duan DD, Zhao D, Zhang ZR: Characterization of cardiac anoctamin1 Ca^{2+}-activated chloride channels and functional role in ischemia-induced arrhythmias. J Cell Physiol 2015;230:337-346.

25 Zhao L, Li LI, Ma KT, Wang Y, Li J, Shi WY, Zhu HE, Zhang ZS, Si JQ: NSAIDs modulate GABA-activated currents via Ca(2+)-activated Cl(-) channels in rat dorsal root ganglion neurons. Exp Ther Med 2016;11:1755-1761.
26 Bernstein K, Vink JY, Fu XW, Wakita H, Danielsson J, Wapner R, Gallos G: Calcium-activated chloride channels anoctamin 1 and 2 promote murine uterine smooth muscle contractility. Am J Obstet Gynecol 2014;211:688 e681-610.
27 Zhang X, Li H, Zhang H, Liu Y, Huo L, Jia Z, Xue Y, Sun X, Zhang W: Inhibition of transmembrane member 16A calcium-activated chloride channels by natural flavonoids contributes to flavonoid anticancer effects. Br J Pharmacol 2017;174:2334-2345.
28 Mazzone A, Eisenman ST, Strege PR, Yao Z, Ordog T, Gibbons SJ, Farrugia G: Inhibition of cell proliferation by a selective inhibitor of the Ca^{2+}-activated Cl^- channel, Ano1. Biochem Biophys Res Commun 2012;427:248-253.
29 De La Fuente R, Namkung W, Mills A, Verkman AS: Small-molecule screen identifies inhibitors of a human intestinal calcium-activated chloride channel. Mol Pharmacol 2008;73:758-768.
30 Hong Y, Cao H, Wang Q, Ye J, Sui L, Feng J, Cai X, Song H, Zhang X, Chen X: MiR-22 may suppress fibrogenesis by targeting TGFbetaR I in cardiac fibroblasts. Cell Physiol Biochem 2016;40:1345-1353.
31 Guo Y, Dong Z, Shi Y, Wang W, Wang L, Sun J, Sun X, Tian Z, Yao J, Li Z, Cheng J, Tian Y: Sonodynamic therapy inhibits fibrogenesis in rat cardiac fibroblasts induced by TGF-beta1. Cell Physiol Biochem 2016;40:579-588.
32 Shinde AV, Frangogiannis NG: Fibroblasts in myocardial infarction: a role in inflammation and repair. J Mol Cell Cardiol 2014;70:74-82.
33 Stauber T, Jentsch TJ: Chloride in vesicular trafficking and function. Annu Rev Physiol 2013;75:453-477.
34 Hwang SJ, Basma N, Sanders KM, Ward SM: Effects of new-generation inhibitors of the calcium-activated chloride channel anoctamin1 on slow waves in the gastrointestinal tract. Br J Pharmacol 2016;173:1339-1349.